# Dynamics of Two-Phase Flow in Porous Media: Simultaneous Invasion of Two Fluids

**Mehrdad Hashemi**
Institute for Theoretical Physics, Cologne University, 50923 Cologne, Germany
Dept. of Chemical Engineering, Amir Kabir University of Technology, Hafez Avenue, Tehran, Iran

**Bahram Dabir**
Dept. of Chemical Engineering, Amir Kabir University of Technology, Hafez Avenue, Tehran, Iran

**Muhammad Sahimi**
Dept. of Chemical Engineering, University of Southern California, Los Angeles, CA 90089

*Models of two-phase flow and displacement in porous media developed so far typically involve one displacing (invader) and one displaced (defender) fluid. However, in many important applications of these phenomena at field scales, such as two-phase flow in fractured porous media, as well as in laboratory studies, require at least two invaders which also act as the defenders. The results of extensive Monte Carlo simulations of a novel model of such phenomena are reported. The porous medium is represented as a network of pore throats and pore bodies to which effective sizes are assigned that are selected from a given distribution. Both 2-D and 3-D networks are used. The simulation results indicate that the structure of the fluids' clusters is volatile, that is, it changes with the time t and length scale. Moreover, $n_s(s,t)$, the number of fluid clusters of size s, $\langle s(t) \rangle$, the mean cluster size, and S(t), the saturation of the fluids all vary with t in a manner that resembles an oscillatory behavior. This behavior is caused by the dynamic breakup and recoalescence of the fluids' clusters, which is a result of simultaneous invasion of the two fluids. The flow effect of thin wetting fluid films on the dynamics of the displacement is strong over a broad range of the capillary number. Novel dynamical scaling laws for the cluster-size distribution are obtained. Some results agree qualitatively with the experimental observations, while others provide rational explanations for some unexplained data.*

## Introduction

Many problems in scientific and industrial fields as diverse as agricultural, biomedical, construction, chemical, and petroleum engineering, food and soil sciences, powder technology, and materials science, involve multiphase flow and displacement processes in a heterogeneous porous medium. These processes constitute a complex set of phenomena that are controlled by several factors, such as the pore space morphology, the interplay between the viscous and capillary forces, the contact angles of the fluids with the surface of the pores, and even the history of the fluid flow. In this article we consider flow and displacement of two immiscible fluids in a disordered porous medium. This process can operate in many modes, such as steady state, imbibition [displacement of a nonwetting fluid (NWF) by a wetting fluid (WF)], drainage (displacement of a WF by a NWF), cocurrent and countercurrent flow of two fluids, among others. In this article, we are concerned with cocurrent flow of two immiscible fluids.

Over the past few decades this phenomenon has been investigated intensively, and a better understanding of it has emerged (for recent reviews see, for example, Sahimi, 1993, 1995). An important controlling parameter is the capillary number, $Ca = \mu v/\gamma$, the ratio of the viscous and capillary forces, where $\mu$ is the fluid viscosity, $v$ its average velocity, and $\gamma$ is the interfacial tension. Experimental observations

Correspondence concerning this article should be addressed to M. Sahimi.
Current address for M. Hashemi: Dept. of Chemical Engineering, Amir Kabir University of Technology, Hafez Avenue, Tehran, Iran.

(for recent experiments, and also for references to the earlier works, see, for example, Avraam et al., 1994; Avraam and Payatakes, 1995) have indicated that over a broad range of the capillary number (and also of several other important parameters of the system) a part of the NWF remains disconnected in the form of clusters or ganglia. The stationary part of the NWF is in the form of stranded clusters, while the moving part of it flows in the form of clusters with a relatively broad size distribution. The moving clusters collide with other clusters and can coalesce with them. Such clusters can also break up into smaller clusters, recoalesce again, and so on. Thus, one has to deal with a variety of complex and interesting phenomena that are sensitive to many parameters of the system, such as those just mentioned. It is this class of phenomena that we discuss in this article.

To investigate these phenomena, pore network models have been used to represent the porous medium in which the sites represent the pore bodies, where most of the fluids reside, and the bonds represent the pore throats through which the fluids flow. For brevity we refer to the pore bodies and pore throats as pores and throats, respectively. Two classes of network models have been developed. In one, the concepts of percolation theory (Stauffer and Aharony, 1992; Sahimi, 1994) have been used for modeling certain aspects of two-phase flow in porous media. These models include random bond or site percolation (see, for example, Larson et al., 1977, 1981; Chatzis and Dullien, 1977, 1985; Kantzas and Chatzis, 1988; Heiba et al., 1982, 1983, 1984, 1992; Sahimi, 1988; Blunt and King, 1991; Bryant and Blunt, 1992; Blunt et al., 1992; Goode and Ramakrishnan, 1993), invasion percolation (see, for example, Lenormand and Bories, 1980; Chandler et al., 1982; Wilkinson and Willemsen, 1983; Furuberg et al., 1988; Birovljev et al., 1991), as well as other models (see, for example, Cieplak and Robbins, 1990; Martys et al., 1991) that have been used for studying the crossover between a percolation-like displacement, which leads to formation of fractal fluid clusters, and one in which the displacing fluid completely sweeps the defending fluid, leading to formation of compact clusters of the invading fluid. Strictly speaking, the percolation models are valid in the limit of very low capillary number $Ca$ (that is, viscous forces are considered unimportant), but in practice the range of their validity may be broader and include moderate values of $Ca$. Moreover, the percolation models cannot by themselves provide any predictions about the dynamics of the motion of the fluid clusters and their interactions with each other. In the second class are more general pore network models in which the details of the interplay between the viscous and capillary forces are included (see, for example, Lenormand et al., 1983, 1988; Dias and Payatakes, 1986a,b; Koplik and Lasseter, 1985; Constantinides and Payatakes, 1991, 1996) and are, in principle, valid for any value of $Ca$. However, percolation concepts have proven useful to even this class model, as they provide a rational way of interpreting the predictions of the models and giving insights into the behavior of the system. Altogether, these models have provided a much deeper understanding of two-phase flow phenomena in porous media. Let us point out that the list of the articles just cited is by no means complete, as there is a vast literature on such models. The interested reader is referred to Sahimi (1993, 1995) for a more complete list of references.

However, most of the models of two-phase flow and displacement in porous media that have been developed so far involve only one displacing (the invader) and one displaced (the defender) fluid, whereas in many typical situations, both at laboratory and field scales, one has to deal with a problem in which there are at least *two* invaders and *two* defenders. We describe here several important examples of this phenomenon that provide the motivation for our work.

### *Measurement of the relative permeabilities*

This problem provides a laboratory-scale example of the class of phenomena that we consider in this article. The relative permeability (RP) $k_{ri}$ to the fluid $i$ is defined by generalizing the Darcy's law to multiphase flow,

$$\boldsymbol{v}_i = -\frac{k}{\mu_i} k_{ri} \nabla P_i, \tag{1}$$

where $\boldsymbol{v}_i$ and $P_i$ are the velocity and the pressure of the fluid $i$, respectively, $\mu_i$ is its viscosity, and $k$ is the absolute permeability of the pore space. In a typical experiment for measuring the RPs (for a detailed discussion see, for example, Avraam and Payatakes, 1995), the porous medium is initially saturated with the NWF (or the WF). Then a *mixture* (not a solution) of the WF and the NWF of a given composition is injected into the sample at a constant flow rate. The two fluids are uniformly distributed at the entrance to the medium, and the flow is maintained until steady state is reached, at which point the pressure drop along the sample is recorded which, together with the flow rates of the two fluids and Eq. 1, yield estimates of the RPs. Thus, measurement of the RPs involves simultaneous invasion of the porous medium by *two* immiscible fluids. An important parameter in such experiments is the fractional flow of a fluid phase $i$ defined as, $f_i = \upsilon_i / \sum_i \upsilon_i$, where the sum is over all the fluid phases present in the porous medium. In this article we study the effect of the fractional flows on the dynamics of the displacement.

### *Enhanced oil recovery by waterflooding*

A popular method of increasing oil production from a reservoir is by waterflooding (Craig, 1971). However, after water injection into an oil reservoir, a considerable fraction of oil is still entrapped in the reservoir. The overall displacement efficiency of the flooding is controlled by both the local and regional sweep efficiencies (defined as the volume fraction of the oil swept by the displacing fluid). To increase the recovery, new production wells are drilled in the regional unswept zones (that is, those areas whose oil has not been displaced and produced), and water is injected at high flow rates into the reservoir through some of the old production wells in the swept regions. To predict the performance of this process, one needs a model for simultaneous flow of both oil and water, because the high flow rate of the water injected into the reservoir causes mobilization toward the producing wells of the oil in the unswept regions, and also of oil and water in the already swept zones. Thus, in this problem one has two invading fluids that also act as the defending fluids in the reservoir.

### *Two-phase flow in rock fractures*

Many natural porous media, such as oil and geothermal reservoirs, and groundwater aquifers, contain fractures at many length scales. Understanding the physics of two-phase flow through fractured porous media is essential to a variety of applied environmental and energy-related problems, such as isolation of high-level radioactive wastes and that of low-level, transuranic, and mixed wastes; environmental restoration; oil recovery from fractured reservoirs (such as those of Iran); and geothermal energy. A comprehensive understanding of these problems requires a detailed examination of what happens in the fractures, both at the level of a single fracture and in the network of the fracture. However, work toward obtaining such an understanding has begun only recently. An important characteristic of a fracture is its aperture $b$, which determines its effective permeability and is defined by, $Q \sim b^{\zeta}$, where $Q$ is the volumetric flow rate in the fracture, and $\zeta$ is a parameter, such that $3 \leq \zeta \leq 6$. The precise value of $\zeta$ for a given fracture depends on the structure of its internal surfaces; for a fracture with smooth internal surface $\zeta = 3$. However, representation of the flow properties of a fracture by only its aperture will lead to gross errors, because a rock fracture is not just a pair of parallel flat plates (as has been assumed in many of the past modeling efforts; for reviews of such efforts see, for example, Sahimi, 1993, 1995) with smooth surfaces (and hence $\zeta = 3$), but a complex network of voids and contact areas and very rough surfaces. Thus, an appropriate model of flow in a single fracture entails representation of the fracture as a network of channels through which a fluid flows (see, for example, Moreno et al., 1988). Once such a representation of a single fracture is accepted, modeling two-phase flow through it becomes similar to that in a porous medium.

Experimental observations in horizontal fractures have indicated (see, for example, Glass and Norton, 1992; Glass and Nicholl, 1995; Glass et al., 1995) that, in two-phase flow through a fracture when an invasion front encounters a zone characterized on average by much smaller apertures (the WF zone) or much larger apertures (the NWF zone), the invading front advances into that region at the expense of the *already invaded region*. In other words, some apertures in the already invaded region are spontaneously reinvaded by the defending fluid to provide invading fluid for the newly encountered zone. In addition, it has been observed that at low flow rates, gravity-driven fingers drain a distance behind the invading fingertip. Thus, two-phase fluid invasion in horizontal fractures involves *simultaneous* imbibition and drainage of the apertures within the fractures.

### *Three-phase flow in porous media*

Another important example of the phenomena that we wish to study in this article is flow of three fluid phases (usually two liquids and a gas) in oil reservoirs (see, for example, Heiba et al., 1984) where, typically, one has three fluid phases—water, oil, and a gas—that might flow simultaneously and try to displace one another. For example, one can have a situation in which the oil is displaced simultaneously by gas and water. Waterflooding in the presence of an evolved gas saturation also belongs to this class of phenomena. The difficulty when three fluid phases are present is that an advancing phase may encounter both pore segments occupied by a second phase and others occupied by a third phase. Therefore, an appropriate model of three-phase flow in a porous medium must take into account simultaneous flow of at least two of the fluids that displace the third fluid and also their own disconnected clusters that may be distributed in the medium.

As can be seen, in all the examples discussed here one has to deal with a multiphase flow problem in a porous medium in which at least two fluids act as the invader and possibly as the defender. However, despite its scientific and practical importance, to our knowledge there has been little attempt to model such phenomena. The purpose of this article is to report the results of a comprehensive study of these phenomena using a new model with two invading and two defending fluids. We show that this model leads to a variety of interesting and complex phenomena that are absent in the models that involve only one invading and one defending fluid. The preliminary results of our model were recently reported in a short article (Hashemi et al., 1998). In the present article we provide the complete details of the model, present extensive new results, and discuss their implications.

This article is organized as follows. In the next section we describe the model and its implementation by computer simulation. We then present extensive results of Monte Carlo simulations of the model, and consider a variety of limiting cases. Next, the universal dynamical properties of the model are investigated briefly. The article is summarized in the last section, where we also discuss extending the model to more complex problems.

## The Model

The porous medium is represented by a square or simple cubic network of throats (bonds) and pores (sites). The throats are assumed to have square cross sections, the effective sizes of which are distributed uniformly in $(0, 1)$; however, any size distribution can be used. The effective sizes of the pores, which must be larger than those of the throats that are connected to them, are assigned by the method described below. Because the problem that we study involves invasion of the porous medium by both the WF and the NWF, we must consider both drainage and imbibition processes. Drainage is relatively simple, and in the context of a pore network model is well understood: The capillary pressure $P_c = P_{nw} - P_w$ is increased slowly and at each value of $P_c$ the NWF advances through the throats with an effective size $r_t$ such that

$$P_c = \frac{2\gamma}{r_t}. \tag{2}$$

Thus, $2\gamma/r_t$ defines a threshold pressure for a throat of size $r_t$. Since the throat sizes are randomly distributed, so also will be the threshold pressures, and therefore one has an irregular interface between the two fluids. Under the quasi-static condition, this process is well-described by invasion percolation, giving rise to the formation of fractal fluid clusters at the breakthrough point, that is, the point at which the NWF cluster spans the network for the first time. We define a NWF

cluster as a set of connected throats that are filled by the NWF fluid.

For imbibition, assignment of the local threshold pressures $P_t$ is much more complex, as they depend not only on the pore space morphology, but also on the fluid configuration, since penetration of a meniscus of a WF into a pore from a throat can modify the effective radius of the pore. Moreover, the WF can flow through the thin films that are attached to the surface of the pores and throats, even if their bulk volume is occupied by the NWF. Thus, unlike the case of NWF, the definition of a WF cluster may not be obvious. Because we include the effect of the thin WF films in the simulation, we define a WF cluster as a set of nearest-neighbor pores (nodes of the network) that are filled by the WF fluid and are connected to each other either by the thin WF films that flow in the crevices of the throats (that is, the corner areas on the walls of the throats with square cross sections) that connect the nearest-neighbor pores, or by the throats themselves if they are filled by the WF fluid.

For imbibition there are several types of displacement mechanisms to be considered. One is pistonlike displacement (flat velocity profile) in the throats, for which the required capillary pressure $P_c$ is given by Eq. 2. A pistonlike displacement in the throats is typically followed by several types of pore filling by the invading fluid, the mechanisms of which depend on the pore's number of nearest-neighbor pores that are already filled with the fluid. For a network of coordination number $Z$, there are $Z$ pore-filling displacement mechanisms, denoted by $\mathfrak{D}_0$ to $\mathfrak{D}_{Z-1}$ (Blunt and Scher, 1995), which represent filling of a pore with 0 to $Z-1$ connecting throats that contain the NWF; see Figure 1. To determine how the displacement proceeds, one needs to calculate the capillary pressure required for each mechanism. In general we know that, $P_c(\mathfrak{D}_0) > P_c(\mathfrak{D}_1) > \cdots > P_c(\mathfrak{D}_{Z-1})$. We also know that the process is limited by the largest radius of curvature necessary to fill the pore, which depends on the number of surrounding throats filled with the invading fluid, and that $\mathfrak{D}_0$ can occur only if the NWF is compressible, since in this case the NWF is trapped in a pore surrounded by throats that are filled by the WF; see Figure 1. However, calculating $P_c(\mathfrak{D}_i)$, and taking into account the effect of the shapes and sizes of the pores and throats as well as the contact angle is very difficult, and even if it were not, it would make the computations prohibitive. Instead of this, we use a parameterization of $P_c(\mathfrak{D}_i)$ for describing the advancement of the fluid, which is as follows. The mean radius of curvature $R_i$ for fill-

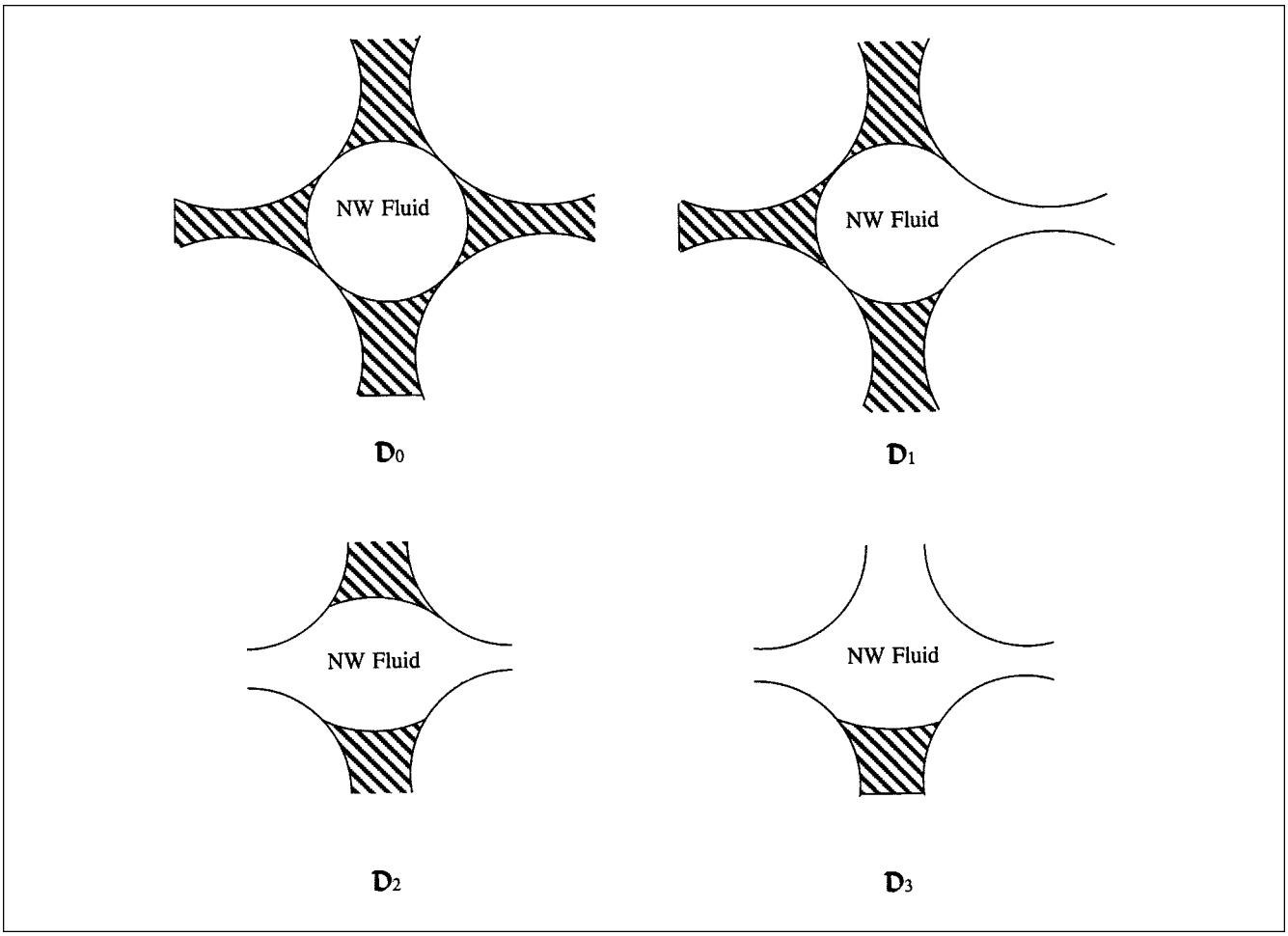


**Figure 1. Several types of pistonlike displacement followed by pore filling.**

Shaded areas represent the WF. Note that in $\mathfrak{D}_0$ the NWF is trapped inside a pore and surrounded by throats that are filled by the WF.

ing by the $\mathfrak{D}_i$ mechanism is (Blunt and Scher, 1995)

$$R_i = R_0 + \sum_{j=1}^{i} A_j x_j, \tag{3}$$

where $x_j$ is a random number distributed uniformly in $(0,1)$, $A_j$ is an input parameter, and $R_0$ is the maximum size of the adjacent throats. The parameters $A_j$, which emulate the effect of the pore-space variables, determine the relative magnitude of the $P_c(\mathfrak{D}_i)$. For example, if for $j \geq 2$ we set $A_j = 0$, then the pore-filling events become independent of the number of the filled throats, and hence the fluid advance is similar to invasion percolation. If, on the other hand, $A_j$ are relatively large for large values of $j$, then the model emulates the case for small or medium values of the ratio of pore and throat radii. In the simulation reported here, $R_i$, as calculated by Eq. 3, is taken to be the pore radius for the $\mathfrak{D}_i$ mechanism of pore filling. Thus, if one fluid is strongly wetting, the critical capillary pressure $P_c$ for pore filling, when the pore has $i$ adjacent unfilled throats, is taken to be

$$P_c = \frac{2\gamma}{R_i}. \tag{4}$$

During imbibition one also has to consider the snap-off mechanism of throat filling (Mohanty et al., 1987): As $P_c$ decreases, the radius of curvature of the interface increases, and the WF films occupying the crevices of the walls swell. At some point further filling of the crevices causes the radius of curvature of the interface to decrease, leading to instability and spontaneous filling of the center of the throat with the WF. The critical capillary pressure for snap-off is given by

$$P_c = \frac{\gamma}{r_t}, \tag{5}$$

which is always smaller than $P_c = 2\gamma/r_t$ for pistonlike displacement. This implies that snap-off can occur only if pistonlike advance is topologically impossible, because there is no neighboring pore filled with the invading fluid. These three displacement mechanisms are included in our imbibition simulations.

Therefore, to simulate imbibition taking into account flow of thin WF films, consider a pore or a throat filled with the NWF, and assume that the WF is provided by thin-film flow along a crevice of length $l$. We ignore any pressure drop in the NWF and in the portions of the network completely saturated by the WF (a valid assumption if the capillary number is small), but the pressure drop along thin wetting layers in the crevices of the network is significant and is not neglected. The relation between the WF flow rate $Q$ and the pressure gradient for the thin films in the corners is

$$Q_f = -\frac{r^4}{\beta\mu_w}\frac{dP_w}{dx}, \tag{6}$$

where $\mu_w$ and $P_w$ are the viscosity and local pressure of the WF, $r$ is the local radius of curvature in the corner, and $\beta$ is a dimensionless conductance factor that depends on the shape of the cross section of the throat and the boundary conditions at the phase boundary. For example (Blunt and Scher, 1995), for square crevices $\beta = 109$, if there is no slip at the interface between the WF and the NWF. More generally, $\beta$ can vary anywhere from 15 to 290 (Ransohoff and Radke, 1988). We assume that locally the interface is in capillary equilibrium and hence $P_w = -P_c = -\gamma/r$. Moreover, we also assume that flow of the thin films (in the crevices) as well as $\beta$ are independent of the time. Then, for the thin films, $Q_f = \gamma^4/(\mu_w \beta P_c^4) dP_c/dx$ (that is, flow of the thin WF films is driven by a capillary pressure gradient in the films). Integrating this equation in $(0, l)$, we obtain

$$P_{c0} = \frac{P_{cl}}{\left(1 + 3\dfrac{\beta P_{cl}^3 Q_f \mu_w l}{\gamma^4}\right)^{1/3}}, \tag{7}$$

where $P_{c0}$ is the capillary pressure of the element (pore or throat) at the inlet of the crevice, and $P_{cl}$ is the local capillary pressure where the element is being filled, either by pistonlike throat filling, or throat filling by snap-off, or by the $\mathfrak{D}_i$ mechanism of pore filling. When the fluid clusters are pushed one after another, $l$ is the minimum distance between the element to be filled, *by the thin WF films*, and the point at the interface between the invading and defending clusters, where the path length through the elements completely filled with the WF is zero. Therefore, when a cluster of the NWF pushes a WF cluster, one has $l = 0$, since there is no path of pores and throats that contain thin films of NWF in the defender cluster; however, $l \neq 0$ when a cluster of the WF pushes a cluster of the NWF, since in this case a thin film of WF can participate in the displacement. If each throat is a channel of radius $r$ and characteristic length $d$ (such as the distance between two neighboring nodes), we rewrite Eq. 7 in dimensionless form by writing $l^* = l/d$, $\mu = Q_f/d^2$, and $P_c^* = P_c r/\gamma$, to obtain

$$P_{c0}^* = \frac{P_{cl}^*}{\left(1 + 3CP_{cl}^{*3} l^*\right)^{1/3}}, \tag{8}$$

where $C = \beta(d/r)^3(u\mu_w/\gamma) = \beta(d/r)^3 Ca$, where $Ca$ is the capillary number for the flow of thin WF films. Assuming that the flow rate in each crevice is constant (independent of the time), we consider the filling of an element with the WF and use Eq. 8, replacing $l$ with the minimum distance between the filling element and the inlet of the filled one, where the path length through the throats completely filled with the WF is zero (that is, only the paths that consist of the thin WF films are counted in calculating $l$).

We first fill the network with the NWF fluid. This represents the initial state of the system at time $t = 0$, after which Monte Carlo simulation of the model begins (the reverse situation in which the network is initially filled with the WF will also be considered; see below). That is, the process starts with an imbibition experiment. The NWF fluid is assumed to be incompressible, and thus its trapping by the WF is possible.

A trapped NWF cluster can be broken up into pieces only by flow of the WF films (see below). We choose at random a site on one face of the network for injection and a site on the opposite face for production. Thus, the boundary condition in the direction of macroscopic displacement is a constant injection rate. We also apply a periodic boundary condition in the other direction(s). The motion of the injected fluid is represented by a series of discrete jumps in which at each time step the invader displaces the defender from the available pores through the least resistance path. In the presence of film flow through the crevices and strongly wetting condition, all the pores are accessible to the WF, while in the case of no film flow, only the interface pores are accessible. At each stage, the pressure needed for flow of the invader from the injection site to the production site through *all the accessible pores* is calculated by summing up the capillary pressure differences of the pores through *all the possible paths* (see below). The path with the least pressure is then selected. This is completely different from the usual fluid-invasion models mentioned earlier, in which only the interface pores are considered. If the WF fluid is displacing the NWF, then after the element is filled, for every possible new path the corresponding $l$ is recomputed (in the case of the NWF displacing the WF, one has $l = 0$). If the number of filled throats adjacent to any of the pores has increased, the pore filling capillary pressures are updated to represent the proper $\mathfrak{D}_i$ mechanism.

The dynamics of fluid displacement that we use here, which is based on finding all the possible paths from the inlet to the outlet of the network, is novel and is not only completely different from the usual invasion models in which only the interface pores and throats are considered, it is also, in our opinion, much more realistic than the previous models of fluid invasion. Because of the complexities that are involved in this model, we now discuss its details.

Consider, for example, a situation in which the NWF is in a cluster that is connected to the inlet of the network and is in contact with three WF clusters, which we call WF1, WF2, and WF3. Suppose that the NWF tries to displace the WF. Since there are three WF clusters that are also in contact with one or several other NWF clusters in ''front'' of them, which in turn touch other NWF clusters, including one that is connected to the outlet of the network, one must consider all the possible paths of the clusters that are pushing one another, and find the path that requires the minimum pressure for the displacement from the point of the contact between the inlet NWF cluster and the outlet of the network. To do this, one must identify all the NWF clusters that are in contact with WF1, WF2, and WF3, which we call the secondary clusters. Then the tertiary clusters that are in contact with the secondary clusters must also be identified, and so on, until all the possible paths from the inlet NWF cluster to the outlet are listed. As such, this is a problem in combinatorial mathematics, which represents a novel aspect of our work.

We then calculate the minimum pressure $\Delta P$ for displacing a WF cluster by a NWF cluster, and vice versa. Consider first the case in which the NWF, which is connected to the inlet of the network, tries to displace a WF cluster. In this case only the elements (pores and throats) of the WF cluster that are at the interface between the two types of clusters are accessible for displacement, as there is no flow of NWF films in any element. Let 1 denote an interfacial element between the invader (in this case the NWF) and the defender cluster (that is, the WF), and 2 denote the outlet point of the WF cluster to another NWF cluster. Recall that the pressure drop between the inlet and the outlet elements is, $\Delta P_{12} = P_{nw1} - P_{w2}$, and that, $P_{nw1} - P_{w1} = P_{c1}$, so that, $\Delta P_{12} = P_{w1} - P_{w2} + P_{c1}$. If we assume that there is no pressure drop in the WF cluster (which is true at low to moderate values of the capillary number $Ca$), then, $\Delta P_{12} \simeq P_{c1}$. Thus, we can calculate $\Delta P_{12}$ for all the interfacial elements between any two NWF and WF clusters that are in contact. Then, for a path that starts from the inlet NWF cluster to the outlet of the network, we write the total required pressure drop $(\Delta P)_{\text{path}}$ as a sum over all such $\Delta P_{12}$ for the NWF and WF clusters that are in contact, being pushed by one cluster on one side (the inlet point 1) and are pushing another cluster at another side (the outlet point 2), and belong to the path:

$$(\Delta P)_{\text{path}} = (\Delta P_{12})_{\text{cluster 1}} + (\Delta P_{12})_{\text{cluster 2}} + (\Delta P_{12})_{\text{cluster 3}} + \cdots = \sum_i (P_{c1})_{\text{cluster } i}, \quad (9)$$

where cluster 1 is in contact with cluster 2, cluster 2 is in contact with cluster 3, and so on. In dimensionless form, each term of Eq. 9 is calculated by using Eq. 8. We then select the path for which $(\Delta P)_{\text{path}}$ is minimum. One has to keep in mind that when a NWF cluster pushes a WF cluster, one must calculate the capillary pressure for all the interfacial elements (that is, all the $P_{c1}$) between the NWF and the WF clusters in order to find the minimum $\Delta P_{12}$.

Now consider the case in which the WF, which is connected to the network inlet, attempts to push a NWF cluster. The general method of selecting the displacement path is the same as before, but two distinct cases have to be considered. One, suppose that there is no flow of thin WF films in the crevices. Using the same arguments and notation as before, it is starightforward to show that for any NWF cluster that is being pushed by the WF and is also pushing another WF cluster, $\Delta P_{12} = -P_{c1}$, assuming again that the pressure in the NWF cluster is the same everywhere. The minimum pressure is again found by considering $(\Delta P)_{\text{path}}$ for all the possible paths. Two, if flow of thin WF films exists, then the WF can reach any part of any cluster of the defending NWF. One must now calculate the minimum $P_c$ for filling *every* element within the NWF cluster, and also those that are at the interface with the WF. Let 1 denote an interfacial element between the invading WF cluster and the defending NWF cluster, 2 be a point inside (a pore of) the NWF cluster, and 3 be the outlet element of the NWF cluster next to another WF cluster. Since the minimum of such $P_c$ corresponds to the minimum $l$ (see Eq. 8), then point 2 is the location of the element within the NWF cluster and 1 is the point at the interface between the WF and NWF that has the smallest distance to that element. We thus have $\Delta P_{13} = P_{w1} - P_{nw3}$ and $P_{c1} = P_{nw1} - P_{w1}$, and therefore, $\Delta P_{13} = P_{nw1} - P_{nw3} - P_{c1}$. Recall that $P_{c1}$ is related to the capillary pressure of the element located at 2 through Eq. 8. Since $P_{nw1} = P_{nw2} = P_{nw3}$, we obtain $\Delta P_{12} = -P_{c1}$. Therefore, in all the cases the individual $\Delta P_{12}$ depend only on the inlet condition of the clusters, and are independent of the outlet conditions. Note that

in both cases, there is a distinct $l$ associated with each possible path. We emphasize that this aspect of our model for fluid cluster mobilization is novel, and is far simpler than the previous models of this phenomenon. Our model reduces this aspect of the problem to one in combinatorial mathematics without any need for explicit flow calculations.

At the end of imbibition, we invade the network with both the WF and the NWF; this initiates the fractional flow displacement (FFD) mentioned in the Introduction. The fraction $f_w$ of the WF in the injected mixture is fixed. At the early stages of FFD, there is a continuous path of the WF through the network, while the NWF remains entrapped in its isolated clusters of ganglia, so that the injected WF can exit from the opposite face of the network, whereas the NWF accumulates in the network. After successive injections, the injected NWF joins its entrapped clusters, and thus larger clusters of the NWF are generated progressively. The invader fluids, both the WF and NWF, push many clusters of the NWF and WF that are already in the network. To calculate the path of the mobilized clusters from the inlet to the outlet, we first identify all the clusters and their adjacent clusters. Then all the possible paths of the clusters from the injection site to the production site are identified and stored in a list. Using Eq. 8 the pressure required to mobilize each of the clusters in the list is calculated for each path. The path that requires the least pressure is selected as the flow path between the inlet and the outlet of the network. Again, this is a novel aspect of our work and represents an important difference between our model for FFD and the usual invasion models in which only the throat with the smallest resistance at the interface is considered. This difference is necessitated by the fact that mobilization of an entrapped fluid cluster is different from simple displacement of one fluid by another in a pore or throat.

We also study the reverse problem in which the network at time $t = 0$ is filled with the WF, and then is invaded by the NWF until the WF becomes disconnected, that is, the process starts with a drainage experiment. A mixture of the WF and the NWF is then injected into the network, and the same procedure as described previously is used for FFD. This is relevant to waterflooding in reservoirs that are oil wet, so that the NWF is water. Finally, we also consider the case in which flow of the thin WF films is neglected, as is customary in the classic models of the two-phase flow and the relative permeabilities.

All of our simulations were carried out with $L \times 2L$ and $L \times L \times 2L$ networks, where $2L$ is the length of the network in the direction of the macroscopic displacement. We varied $L$ as one parameter of the model to study its effect on the results. We also averaged the simulation results over up to 100 realizations of the network. In the following discussion, time is measured in terms of the number of the elementary displacement events. Since we do not carry out explicit calculations to compute the pressure fields in the bulk of the two fluids, the actual time is not computed.

## Results and Discussion

We have carried out extensive Monte Carlo simulations of the model in both 2-D and 3-D networks. Use of both 2-D and 3-D networks is necessitated by the fact that there are subtle differences between two-phase flow in 2-D and 3-D systems. Another goal of the comparison between the two cases is to understand those aspects of the problem that depend on, or are independent of, the dimensionality of the system. We first present the results for 2-D networks, and then discuss the 3-D results. We consider three distinct cases. In the first case FFD is preceded by imbibition of the WF into the porous medium, while in the second case the system at time $t = 0$ is filled by the WF and is invaded by the NWF, that is, a drainage experiment. Finally, in the third case we discuss briefly the case in which flow of the thin WF films is ignored. Since we are mainly interested in the dynamics of the displacement process, we focus on the time dependence of three important properties, namely, $n_s(s, t)$, the number of fluid clusters of size $s$ at time $t$, $\langle s(t) \rangle$, the mean cluster size at time $t$, and $S(t)$, the fluid saturation at time $t$, where a time step is defined as an attempt to fill a pore or a throat. We study these three quantities for both fluids for all the displacement processes that are considered here.

### *Results with two-dimensional networks*

*Imbibition Followed by Fractional Flow Displacement.* Figure 2 shows snapshots of the system during three stages of FFD in a $100 \times 200$ square network for various values of $C$ and $f_w = f_{nw} = 0.5$. It is clear that flow of the WF films plays a major role in the displacement process at low $C$, since the films invade small pores filled with the NWF that are far from the interface. Moreover, the effect of $C$ is quite pronounced as the patterns change considerably with increasing $C$. Interestingly, although due to the flow of the thin WF films during imbibition the WF is always sample spanning and continuous, there is no sample-spanning cluster of the *pores* that is filled with the WF, even at the final stage of the displacement. Since before FFD begins the NWF has been displaced by an imbibition process, at early stages of FFD clusters of the NWF are isolated, but as FFD proceeds they become connected progressively and form larger clusters. At some point during FFD both the fluid phases become continuous, the NWF via the sample-spanning cluster of the pores and throats that it occupies, and the WF through the thin films and the pores that it has invaded. This is a novel feature of FFD in 2-D with flow of thin films, and is in contrast with the previous models of fluid invasion in which there is only one continuous fluid phase during the displacement. Our simulations indicate that the displacement reaches the steady-state condition only after a long time, at which time it becomes a steady-state dynamic displacement process.

The time dependence of $n_s(s, t)$, the number of fluid clusters of size $s$ at time $t$, during FFD is shown in Figures 3 and 4. [In all the cases discussed here, for the sake of clarity, we do not normalize $n_s(s, t)$ by the volume of the network, either $2L^2$ in 2-D or $2L^3$ in 3-D, which is the standard practice in network simulations.] Figure 3a presents the results for the NWF for $f_w = 0.5$, $C = 10^{-5}$, and a few values of $s$, while Figure 3b presents the same for $C = 10^{-1}$. These results demonstrate that $n_s(s, t)$ fluctuates, or, roughly speaking, oscillates aperiodically, with time $t$. The oscillations are *not* statistical noise in the Monte Carlo data, as the results present an average over many realizations of the network. They are caused by the volatile nature of the fluid clusters: the

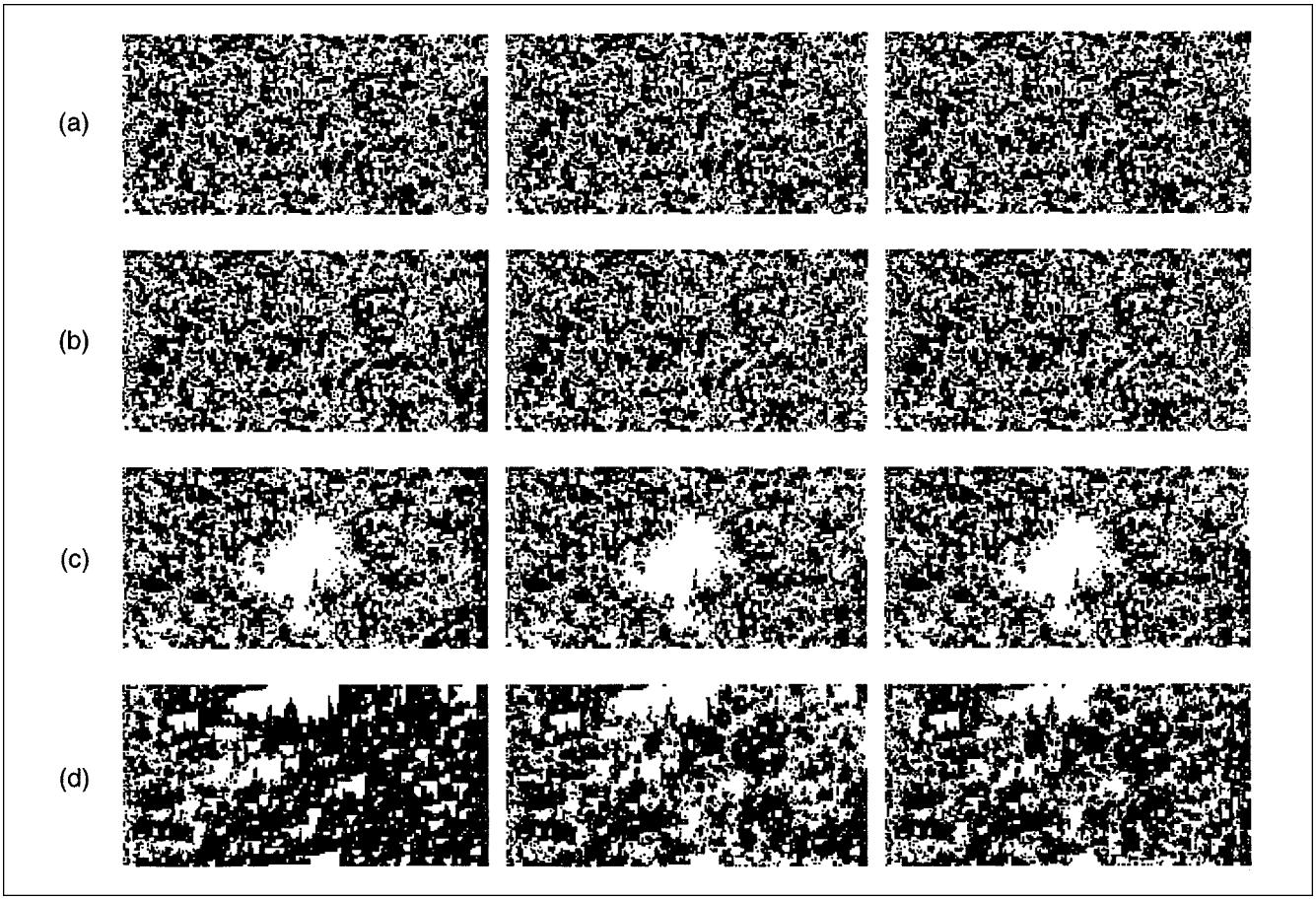


**Figure 2. Snapshots of the 2-D system during FFD preceded by imbibition for $f_w = 0.5$, and (a) $C = 10^{-5}$; (b) $C = 10^{-3}$; (c) $C = 10^{-2}$; (d) $C = 10^{-1}$.**

Black and white areas represent the WF and the NWF, respectively. Time increases from left to right, from $t = 5{,}000$ to 10,000, and 15,000.

clusters break up continuously by the invasion of the WF films, but they also recoalesce as the displacement proceeds and smaller fluid clusters rejoin. This implies that at different length scales the clusters change their identity. Moreover, as we show below, the oscillations persist even when the network size becomes large, indicating again that they have a physical origin. We note that for $C = 10^{-5}$ the fluctuations in the number of relatively large clusters is very small. A com-

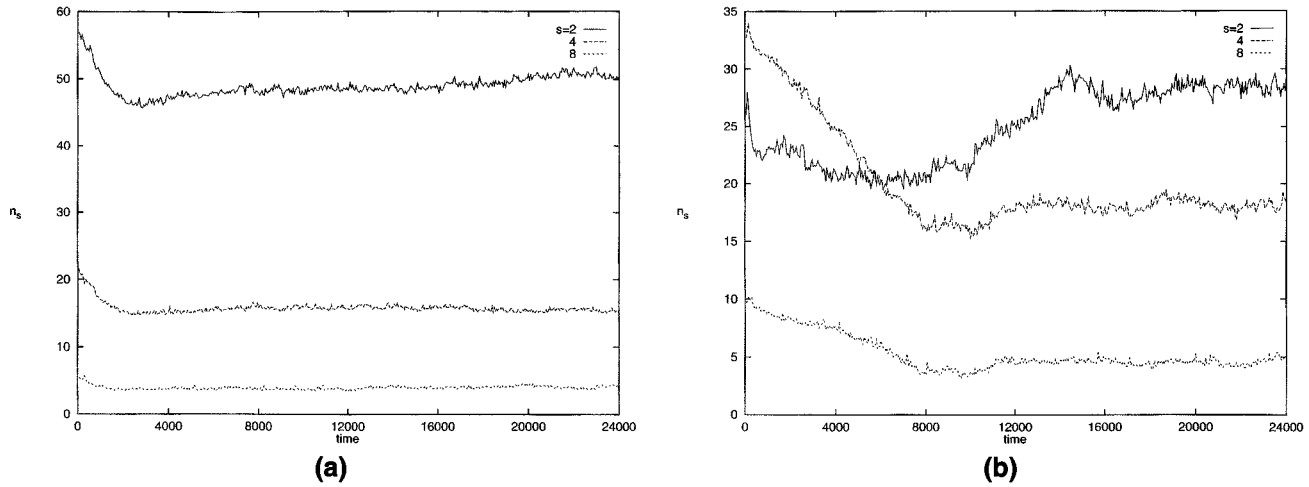


**Figure 3. Time dependence of the cluster size distribution $n_s(s,t)$ for the NWF during FFD in the square network preceded by imbibition for $f_w = 0.5$, and (a) $C = 10^{-5}$; (b) $C = 10^{-1}$.**

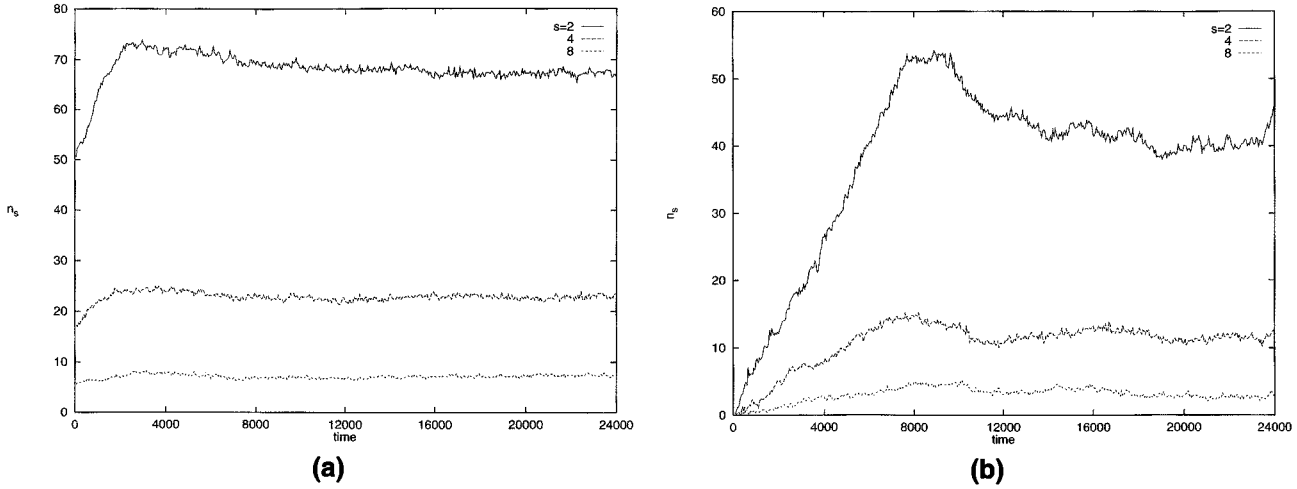


**Figure 4. Time dependence of the cluster size distribution $n_s(s,t)$ for the WF during FFD in the square network preceded by imbibition for $f_w = 0.5$, and (a) $C = 10^{-5}$; (b) $C = 10^{-1}$.**

parison between Figures 3a and 3b indicates that, with increasing *Ca* the oscillations in $n_s(s,t)$ also increase, because it becomes in some sense easier to break up larger fluid clusters. This assertion is also supported by the fact that the fluctuations of $n_s(s,t)$ for larger values of $s$ also increase as *Ca* does. Moreover, as Figures 3a and 3b both indicate, for larger values of $C$, the number of larger clusters increases, while that of smaller clusters decreases. This is also evident in the displacement patterns shown in Figure 2.

Qualitatively similar results are obtained for the WF. Figures 4a and 4b present the results for the WF under the same conditions as in Figures 3a and 3b. However, there are two major differences between the results for the WF and the NWF. One is that, as Figures 4a and 4b indicate, the amplitude of the oscillations for the WF is smaller than that of the NWF. This is caused by the fact that flow of the thin WF films cannot affect the structure of its clusters. Thus, for the WF the oscillations are only due to the collisions between its clusters and their coalescence for forming larger clusters, which can be broken up again by the invading NWF. The second difference between the behavior of the two fluids is that, as Figures 4a and 4b indicate, for the WF $n_s(s,t)$ reaches a maximum, whereas for the NWF no particular pattern is seen for $n_s(s,t)$, since the NWF clusters can be broken up by flow of the thin WF films anywhere in the network.

The oscillations can be understood better if one studies the mean cluster size $\langle s(t)\rangle$, defined by

$$\langle s(t)\rangle = \frac{\sum_s s^2 n_s(s,t)}{\sum_s s n_s(s,t)}. \qquad (10)$$

Figure 5 presents the results for $\langle s_{nw}(t)\rangle$, the mean size of the NWF clusters normalized by the volume $2L^2$ of the network, during FFD for two values of $C$ and $f_w = 0.5$. Although the mean cluster size represents an averaged quantity in which the averaging has been taken over all the NWF clusters and many realizations of the network, there are still large oscillations. As Figure 5 indicates, $\langle s_{nw}(t)\rangle$ increases rapidly at the early stages of FFD, but, similar to $n_s(s,t)$, after some time $t$ it starts to oscillate widely, with the oscillations being particularly strong for $C = 10^{-1}$. Figure 6 shows the same results for the WF. In contrast with the NWF, $\langle s_w(t)\rangle$, the mean cluster size of the WF *decreases* to about one-third of its initial value and then oscillates with $t$ with an amplitude that is *smaller* than that of the NWF because, as discussed earlier, flow of the thin WF films has no effect on the WF clusters. These features of our model, which persist over a wide range of $C$ and any value of $f_w$, cannot be predicted by the usual fluid-invasion models with one invader and one defender.

In experimental studies of two-phase flow in porous media, a quantity of prime interest, which can be measured directly, is the saturation of a fluid phase, that is, the volume fraction of the pore space occupied by the fluid phase. Figure 7 presents the time dependence of the saturation $S_{nw}$ of the NWF. Because the saturation of a fluid phase is proportional to its total number of clusters in the pore space, one expects $S_{nw}$

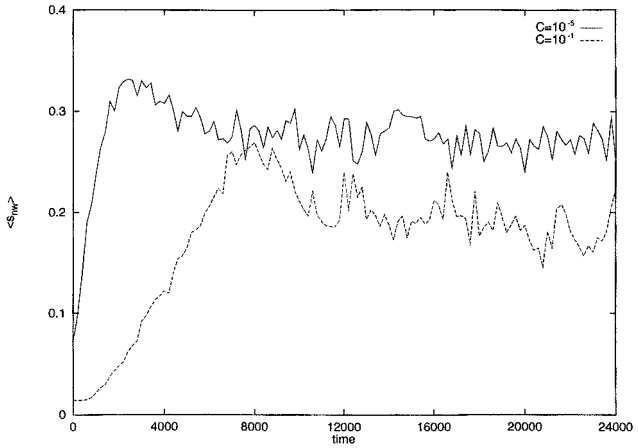


**Figure 5. Time dependence of the mean cluster size $\langle s_{nw} rangle$ of the NWF during FFD in the square network preceded by imbibition for $f_w = 0.5$.**

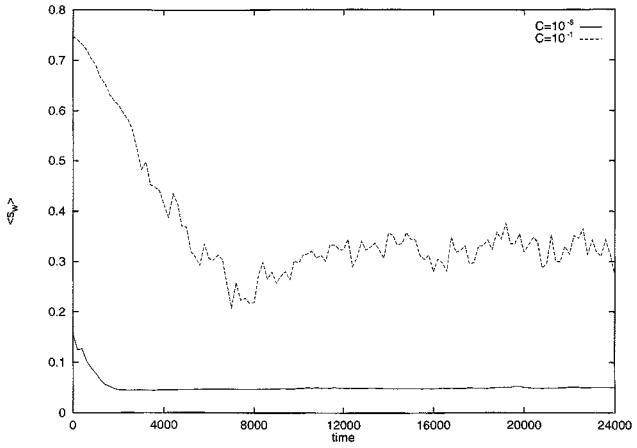


**Figure 6. Time dependence of the mean cluster size $\langle s_w \rangle$ of the WF during FFD in the square network preceded by imbibition for $f_w = 0.5$.**

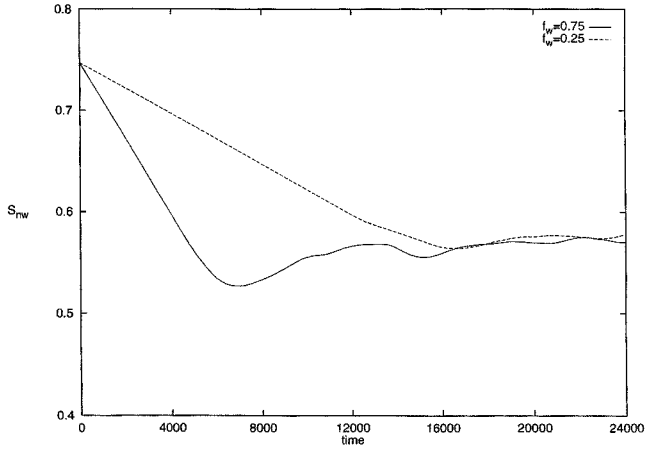


**Figure 7. Time dependence of the saturation $S_{nw}$ of the NWF during FFD in the square network preceded by imbibition.**

to fluctuate with the time $t$, and Figure 7 confirms this expectation. Such fluctuations and oscillations have often been observed in experiments (Craig, 1971; Avraam and Payatakes, 1995), but have been mostly attributed to the uncertainty in the measurements, whereas as our simulations demonstrate, they have a clear physical origin and cannot be dismissed as experimental uncertainties. This point was also emphasized by Avraam and Payatakes (1995). Because the relative per-

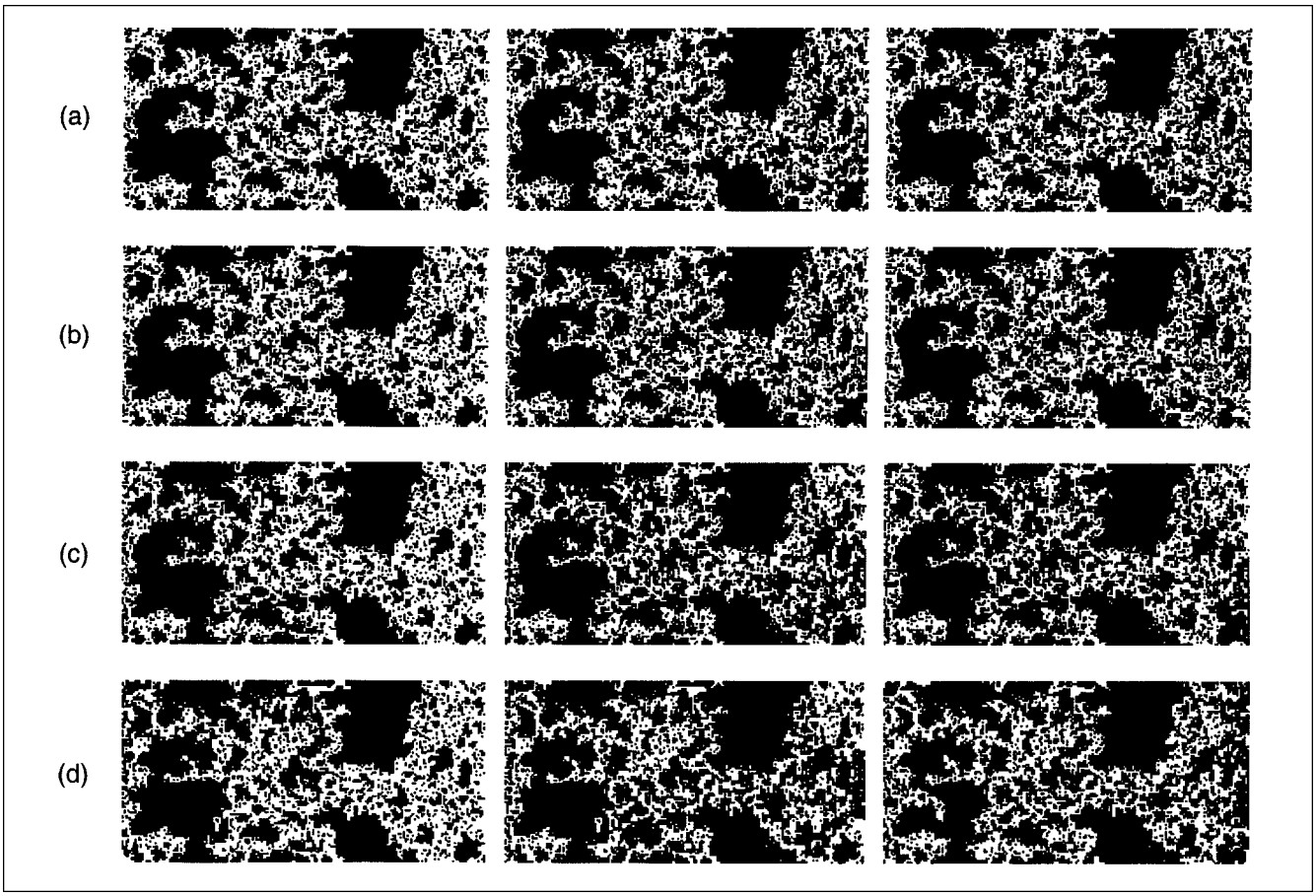


**Figure 8. Snapshots of the 2-D system during FFD preceded by drainage for $f_w = 0.5$, and (a) $C = 10^{-5}$; (b) $C = 10^{-3}$; (c) $C = 10^{-2}$; and (d) $C = 10^{-1}$.**

Time increases from left to right.

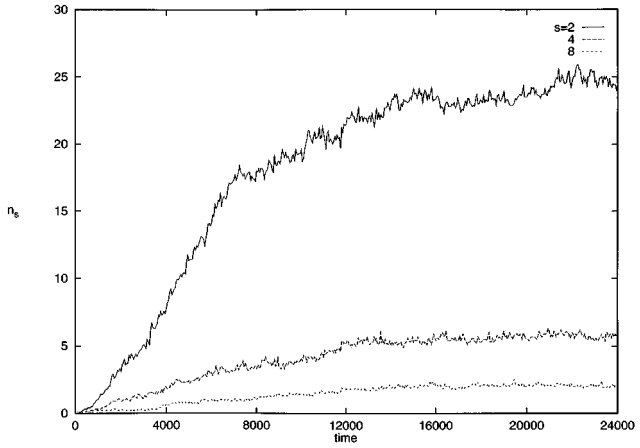


**Figure 9. Time dependence of the cluster size distribution $n_s(s,t)$ for the NWF during FFD in the square network, preceded by drainage for $C = 10^{-5}$ and $f_w = 0.5$.**

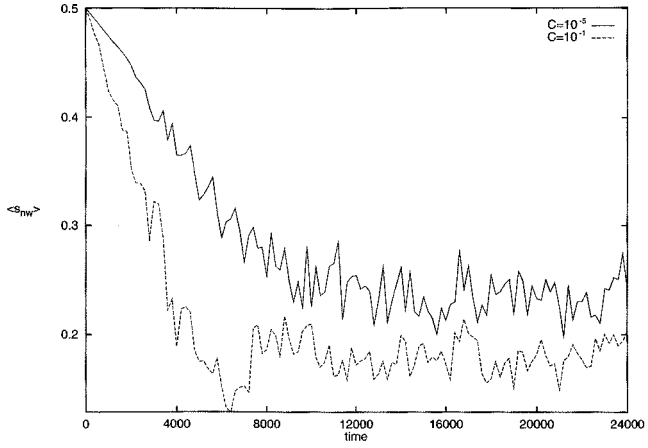


**Figure 11. Time dependence of the mean cluster size $\langle s_{nw}(t) \rangle$ of the NWF during FFD in the square network preceded by drainage for $f_w = 0.5$.**

meabilities depend strongly on the saturations, we expect them to also fluctuate with the process time. Indeed, using a completely different model, Constantinides and Payatakes (1996) found such oscillations in their calculated relative permeabilities. Therefore, a proper definition of the relative permeabilities must involve an average over the time period in which they are measured. Otherwise, the relative permeabilities will be time-dependent quantities.

*Drainage Followed by Fractional Flow Displacement.* Figure 8 presents the snapshots of the network during FFD for four values of $C$. The displacement patterns are completely different from those shown in Figure 2, which are for a system in which FFD was preceded by imbibition. The reason for this difference is as follows. Because the present FFD starts at the end of a drainage experiment when the WF is mostly in isolated clusters of small pores and throats, flow of the thin WF films is not effective and cannot have a strong influence on the displacement patterns. Therefore, unlike the displacement patterns of Figure 2, varying $C$ does not change greatly the dynamics of the process. As a result, the displacement patterns shown in Figure 8 resemble to some extent those that are obtained with the invasion percolation model which does not (and cannot) take into account the effect of the thin WF films.

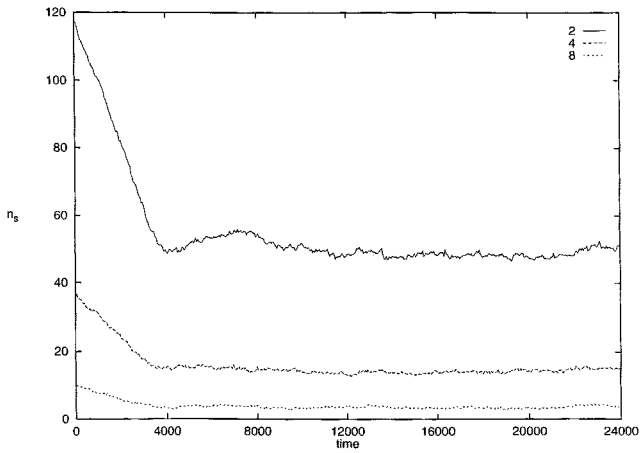


**Figure 10. Time dependence of the cluster size distribution $n_s(s,t)$ for the WF during FFD in the square network, preceded by drainage for $C = 10^{-1}$ and $f_w = 0.75$.**

Because flow of the thin WF films is not very effective, we expect to see qualitative differences between the cluster-size distribution $n_s(s,t)$ of the fluids in the present case and the FFD that was preceded by imbibition (see earlier). For example, Figure 9 presents the fluid cluster-size distributions for the NWF for $f_w = f_{nw} = 0.5$ and $C = 10^{-5}$, which are quite different from those shown in Figures 3a and 3b. Because the present FFD begins at the end of drainage, we expect to have a relatively small number of the NWF clusters in the system, and Figure 9 confirms our expectation. On the other hand, for the WF fluid we expect to have the initial number of the clusters decrease sharply, because in the initial stages of FFD the flow of the WF helps join the isolated clusters of the WF, and then fluctuate with the time. This is confirmed by the results shown in Figure 10 for the cluster-size distribution of the WF for $f_w = 0.75$ and $C = 10^{-1}$, which should be compared with those shown in Figure 4b. The ineffectiveness of the flow of the thin WF films also affects the behavior of the mean cluster size. Shown in Figures 11 and 12 are the mean cluster sizes for the two fluids, which are very different from those in Figures 5 and 6. These results demonstrate the significance of the thin WF films to the dynamics of the displacement processes. Furthermore, they point out the importance of the initial displacement mode, imbibition or drainage, to FFD. In the classic models of two-phase flow and displacement in porous media, which are based on continuum equations of fluid flow, the effect of the flow of the WF films is generally neglected, perhaps because taking into account such an effect is very difficult within the framework of such models.

### *Results with three-dimensional networks*

In this section we present the results with the simple cubic network. As in the 2-D case, we discuss the FFD results for

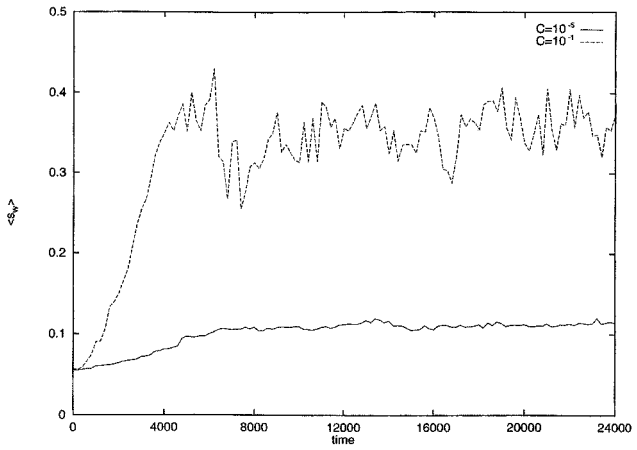


**Figure 12. Time dependence of the mean cluster size $\langle s_w(t) \rangle$ of the WF during FFD in the square network preceded by drainage for $f_w = 0.5$.**

two distinct cases, namely, imbibition followed by FFD, and drainage followed by FFD. Most of our results were obtained with $25 \times 25 \times 50$ networks.

*Imbibition Followed by Fractional Flow Displacement.* In Figures 13a, 13b and 13c we present the cluster-size distributions for the NWF during FFD, which was preceded by imbibition for $C = 10^{-5}$ and three values of $f_w$. Unlike their two-dimensional counterparts shown in Figures 3a and 3b, the cluster-size distribution does not exhibit large fluctuations. In all the cases, $n_s(s,t)$ increases initially to reach a maximum, after which it decreases with the process time. After about 20,000 time steps, the cluster-size distribution of the fluid changes very little with $t$. This behavior persists over a broad range of $C$. However, the WF does not exhibit the same behavior. Shown in Figures 14a, 14b, and 14c are the results for the WF for the same sets of parameters as those of Figure 13. At the lowest value, $f_w = 0.25$ (Figure 14a), the cluster-size distribution increases sharply with the process time with relatively large fluctuations. Although after about

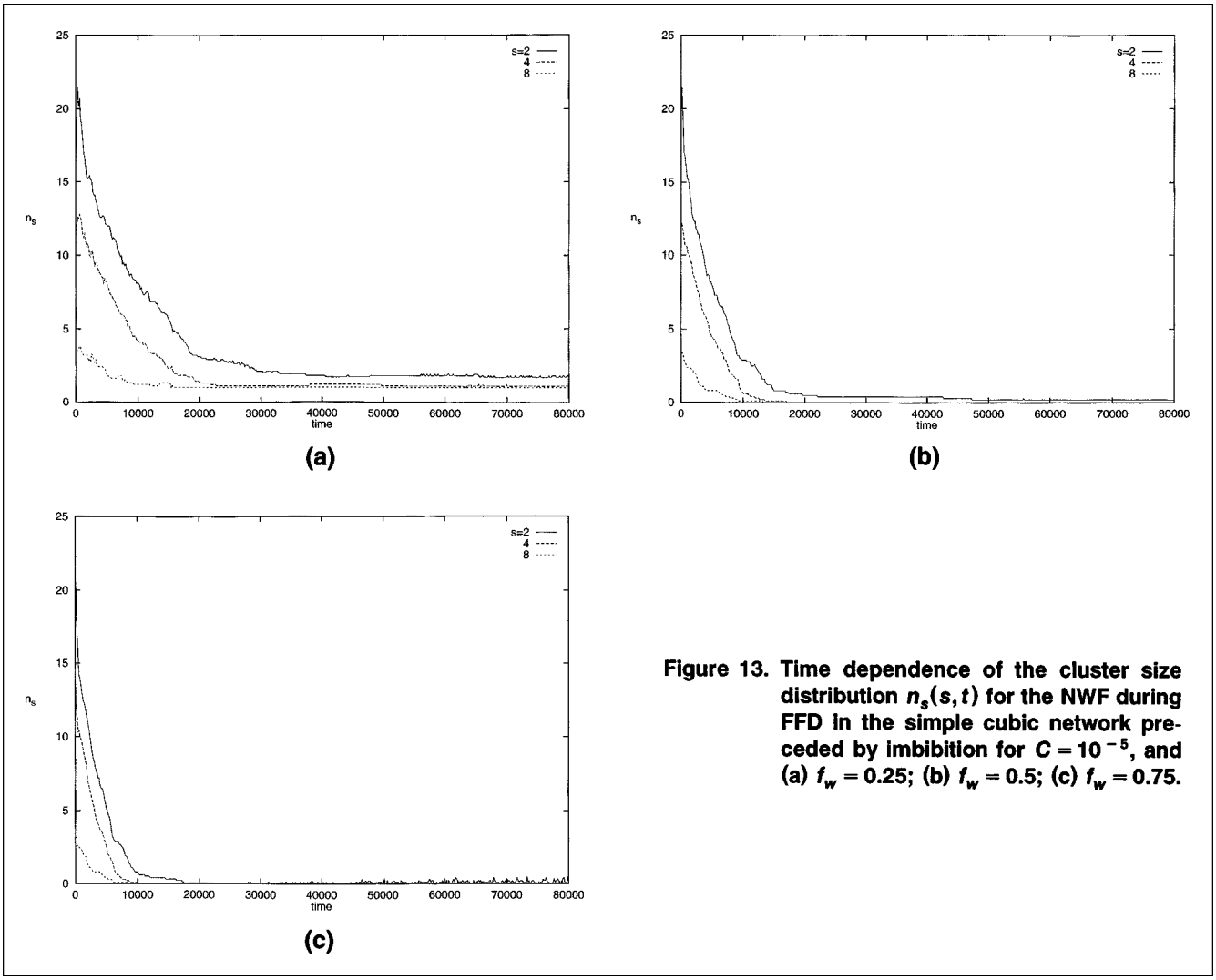


**Figure 13. Time dependence of the cluster size distribution $n_s(s,t)$ for the NWF during FFD in the simple cubic network preceded by imbibition for $C = 10^{-5}$, and (a) $f_w = 0.25$; (b) $f_w = 0.5$; (c) $f_w = 0.75$.**

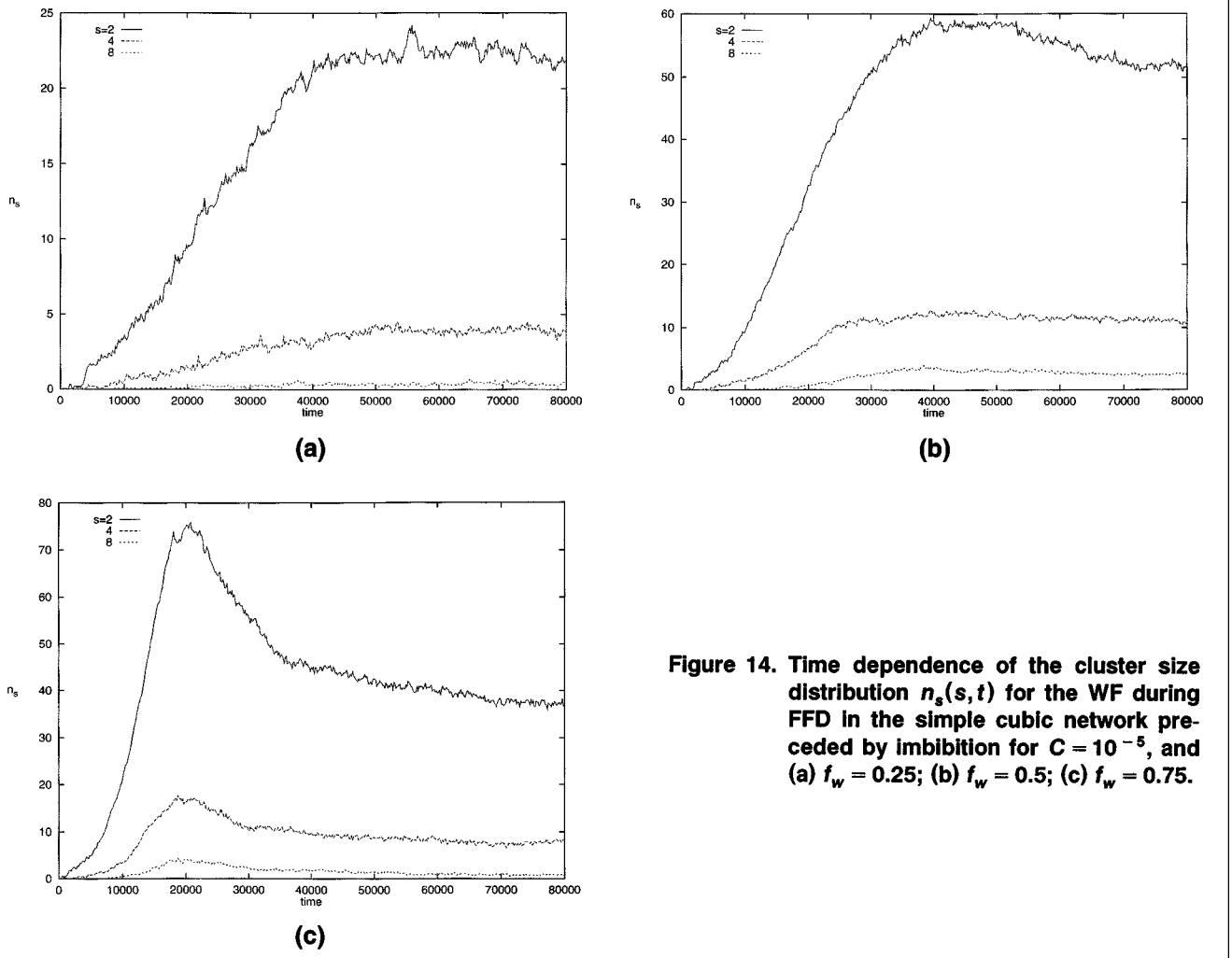


**Figure 14. Time dependence of the cluster size distribution $n_s(s,t)$ for the WF during FFD in the simple cubic network preceded by imbibition for $C = 10^{-5}$, and (a) $f_w = 0.25$; (b) $f_w = 0.5$; (c) $f_w = 0.75$.**

40,000 time steps $n_s(s,t)$ appears to have reached a sort of quasi-steady state, the aperiodic oscillations persist. As $f_w$ increases, two notable features emerge. First, similar to the NWF case, $n_s(s,t)$ starts to exhibit a maximum and, second, the amplitude of the oscillations decreases somewhat. This behavior persists over a broad range of $C$. For example, Figure 15 shows the results for $f_w = 0.25$ and $C = 10^{-1}$ which, when compared with Figure 14a, indicates the same type of behavior, except that in this case the oscillations are even stronger than those at $C = 10^{-5}$.

The difference between the results for 2-D and 3-D networks is striking, and may be explained as follows. If we ignore flow of the thin WF films, then a bicontinuous structure in which both WF and NWF are sample spanning cannot exist in 2-D, whereas this possibility does exist in 3-D. Thus, in 3-D the invading fluids can go around the clusters of the defending fluids and find their way in the network until they form a sample-spanning cluster, because this requires a smaller $(\Delta P)_{\text{path}}$, whereas because of topological (dimensional) restriction this is not possible in 2-D. As a result, while

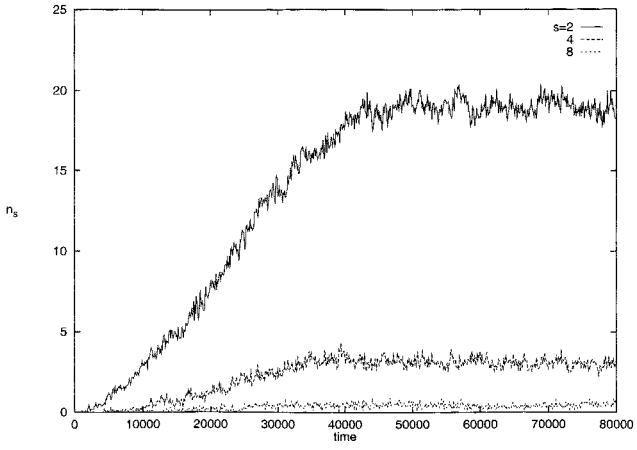


**Figure 15. Time dependence of the cluster size distribution $n_s(s,t)$ for the WF during FFD in the simple cubic network preceded by imbibition for $C = 10^{-1}$ and $f_w = 0.25$.**

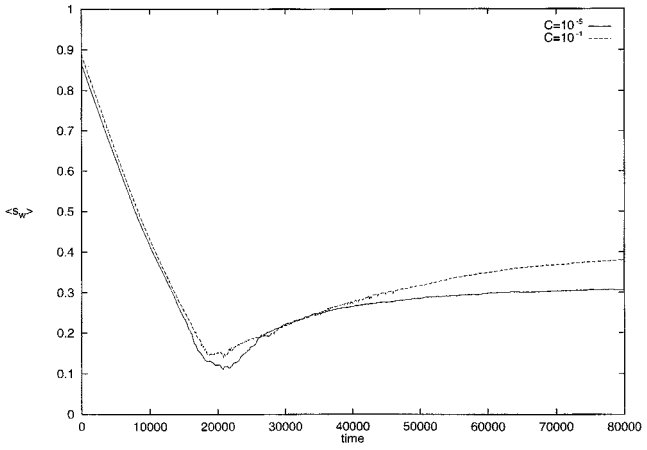


**Figure 16. Time dependence of the mean cluster size $\langle s_w(t) \rangle$ of the WF during FFD in the simple cubic network preceded by imbibition for $f_w = 0.75$.**

in 2-D the fluid clusters are continuously displacing some clusters and are also being displaced by other clusters, the same is not true in 3-D. Therefore, in our model breakup and recoalescence of the fluid clusters in 2-D is far more frequent than in 3-D. This reasoning is true as long as the effect of the viscous forces is neglected, which is the case in our model except in the thin WF films. If viscous forces are explicitly taken into account [this requires calculations of the flow fields within the two fluid phases (see, for example, Constantinides and Payatakes, 1996)], then 2-D and 3-D systems will be much more similar. Work in this direction is currently in progress.

Figures 16 and 17 present the mean cluster sizes $\langle s_w(t) \rangle$ and $\langle s_{nw}(t) \rangle$ during FFD for $f_w = 0.75$ and two values of $C$. The mean cluster sizes have been normalized by the volume $2L^3$ of the network. Because fluctuations of the cluster-size distributions in 3-D are not as strong as those in 2-D, then, consistent with our discussion, the mean cluster sizes are essentially smooth. However, while $\langle s_{nw}(t) \rangle$ reaches a maximum and then starts to slowly decrease, $\langle s_w(t) \rangle$ exhibits the opposite trends. This difference is, of course, caused by the fact that the FFD was preceded by drainage at the end of which the NWF exists only in a large number of small clusters. Therefore, at the beginning of FFD the invading NWF helps connect such clusters and thus $\langle s_{nw}(t) \rangle$ increases. After some time FFD reaches a quasi-steady state and therefore the mean cluster size varies very slowly with the process time.

*Drainage Followed by Fractional Flow Displacement.* The results for this case are similar to what we discussed for the case in which FFD was preceded by imbibition. Because in the present case FFD begins at the end of drainage when the WF exists only in isolated clusters, we expect to have the largest fluctuations in the cluster-size distribution of the WF, and this is indeed the case. Shown in Figures 18a and 18b are the results for $C = 10^{-1}$ and two values of $f_w$. The cluster-size distribution exhibits large fluctuations in both cases. Similar results are obtained for the NWF, and thus are not shown here.

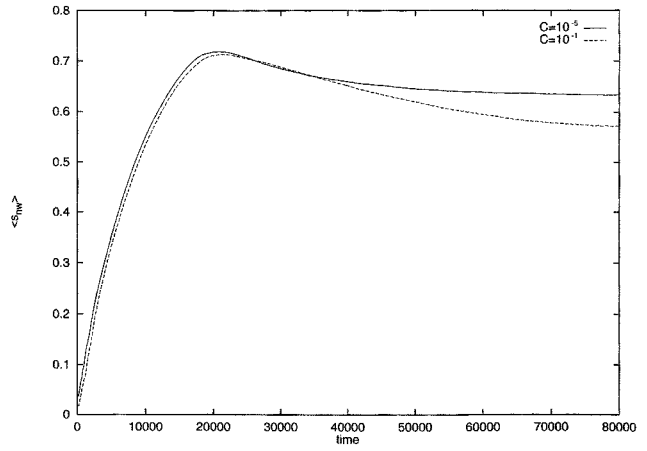


**Figure 17. Time dependence of the mean cluster size $\langle s_{nw}(t) \rangle$ of the NWF during FFD in the simple cubic network preceded by imbibition for $f_w = 0.75$.**

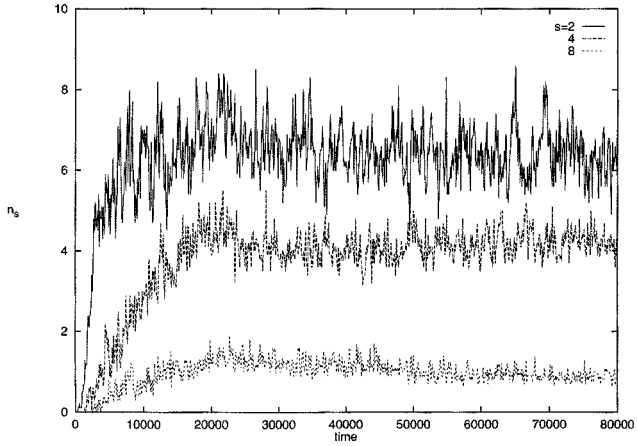


**(a)**

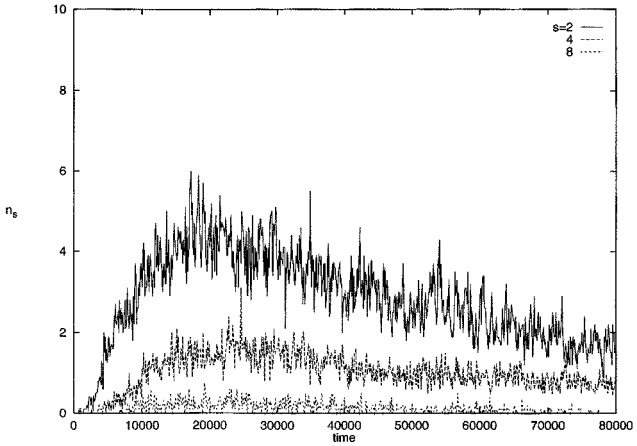


**(b)**

**Figure 18. Time dependence of the cluster size distribution $n_s(s,t)$ for the WF during FFD in the simple cubic network preceded by drainage for $C = 10^{-1}$, and (a) $f_w = 0.25$; (b) $f_w = 0.75$.**

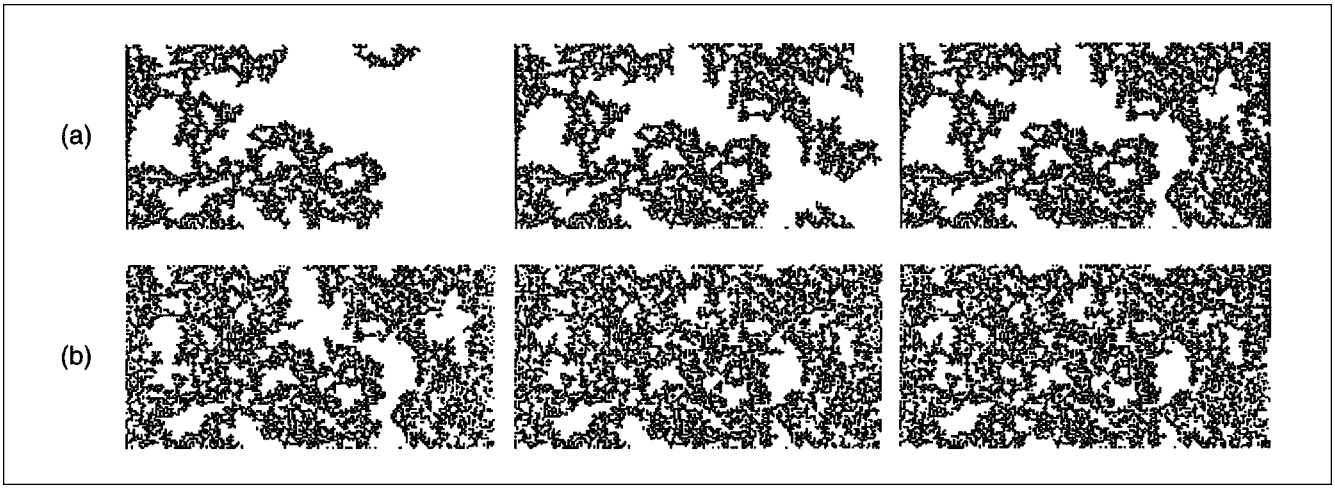


**Figure 19. Snapshots of displacement patterns in the 2-D network during (a) imbibition, and (b) FFD after the imbibition for $f_w = 0.5$, in which flow of the thin WF films has been neglected.**

### *Fractional flow displacement without flow of thin wetting films*

As discussed earlier, in the continuum models of two-phase flow, the relative permeabilities, and FFD, the effect of flow of thin WF films is neglected, and thus it is of practical interest to compare the results discussed previously with those for a system in which this effect has been neglected completely. This allows us to test the accuracy of the continuum models in neglecting the thin wetting films. Figure 19 presents snapshots of the 2-D system during imbibition followed by a FFD, indicating that the displacement patterns in this case are much different from those with film flow that are shown in Figure 2. This large difference between the two cases indicates the significance of the flow of the thin WF films. More quantitatively, the difference between the two processes manifests itself in the mean cluster-size distribution. For example, Figure 20 presents $\langle s_{nw}(t)\rangle$ during a FFD that is preceded by imbibition or drainage, which should be compared with those shown in Figure 5, indicating different qualitative as well as quantitative behavior. We can conclude that the flow of thin WF films, which is neglected in the classic computations of the relative permeabilities and FFD, affects significantly the displacement process and cannot be neglected.

### *Dependence of the residual saturation on the capillary number*

An important parameter in enhanced oil recovery is the residual saturation $S_{or}$ of the NWF (say, oil), which is its saturation at the end of imbibition when the NWF is only in the form of isolated clusters. In general, $S_{or}$ depends on the capillary number, and is also strongly affected by flow of thin WF films that expel the NWF from the pores. Figure 21 presents the predictions of our model for $S_{or}$ as a function of the capillary number for two network sizes, indicating that $S_{or}$ is

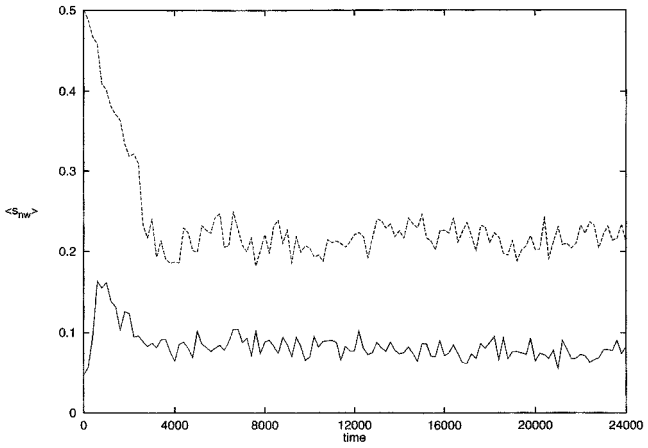


**Figure 20. Time dependence of the mean cluster size for the NWF during FFD with $f_w = 0.5$ in the square network preceded by imbibition (solid line) and by drainage (dashed line), without flow of the thin WF films.**

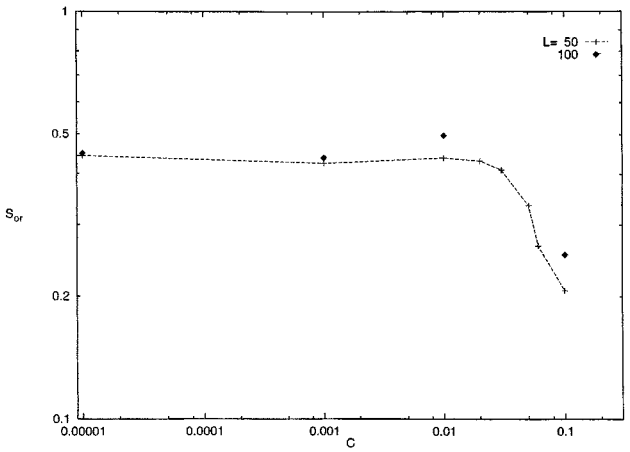


**Figure 21. Dependence of the residual oil saturation $S_{or}$ on the capillary number $C$ in $L \times 2L$ networks with $L = 50$ (+) and $L = 100$ (diamonds).**

essentially independent of the capillary number until it reaches a critical value, which is about $Ca = 10^{-2}$, beyond which it decreases sharply with $Ca$. These features are in excellent qualitative agreement with the experimental data (see, for example, Sahimi, 1995, p. 345), and lend further support to validity of our model.

### *Universal scaling properties of the displacement processes*

The fluctuations and oscillations that are predicted by our model are absent in random and invasion percolation models with one invading and one defending fluid. In these models the fluid cluster-size distribution obeys a universal scaling law that is independent of many microscopic features of the model. In our model with two invading and two defending fluids, *despite* the fluctuations and oscillations of the cluster size distribution with the time $t$, $n_s(s,t)$ still follows a universal scaling law for both the WF and NWF. In percolation and similar models one usually has the following scaling law for the cluster-size distribution

$$n_s(s,t) \sim s^{-\tau} f[s(t)/\langle s(t)\rangle], \tag{11}$$

where $f(x)$ is a scaling function, and $\tau$ a universal exponent. However, in our model, because of the fluctuations and oscillations of $n_s(s,t)$ with $t$, a better way of studying the cluster statistics is by investigating $N_s = \Sigma n_s$, the total number of clusters with a size greater than a given size $s$. If we replace $\Sigma$ by an integral and use Eq. 11, we obtain

$$N_s \sim s^{1-\tau} f[s(t)/\langle s(t)\rangle]. \tag{12}$$

The scaling function $f(x)$ has a power-law decay $f(x) = x^{-y} g(x)$, with $g$ being a cutoff function that decays exponentially for $x > 1$. Moreover, because, as discussed earlier, the fluid clusters are volatile, that is, change their identity with the length scale, $N_s$ should depend on the size of the network. We find that this is indeed the case, and that $N_s$ obeys simple and elegant scaling laws. At any fixed time $t$ during FFD, we can collapse the results for $N_s$ obtained with different network sizes $L$ according to

$$\frac{N_s(L;t)}{s} \sim \langle s(t)\rangle^{-2} g[s(t)/\langle s(t)\rangle]. \tag{13}$$

For example, Figure 22 presents the results of such a data collapse for the WF at a fixed intermediate time, $t = 10{,}000$, during FFD in the square network that was preceded by imbibition, with $f_w = 0.25$ and $C = 10^{-5}$, indicating very accurate data collapse over much of the range of $s/\langle s\rangle$.

Let us emphasize an important point regarding Eq. 13. That one obtains universal dynamical scaling (Eq. 13) with the network size $L$ is a novel confirmation of the fact that the aperiodic oscillations are not merely Monte Carlo noise, because otherwise one must obtain two different scaling laws, one for small $L$, where the noise is very strong, and another one for large $L$, where the oscillations should presumably vanish if they represent only the noise in the Monte Carlo data. However, as Figure 22 demonstrates, one obtains only a single scaling law valid for any $L$.

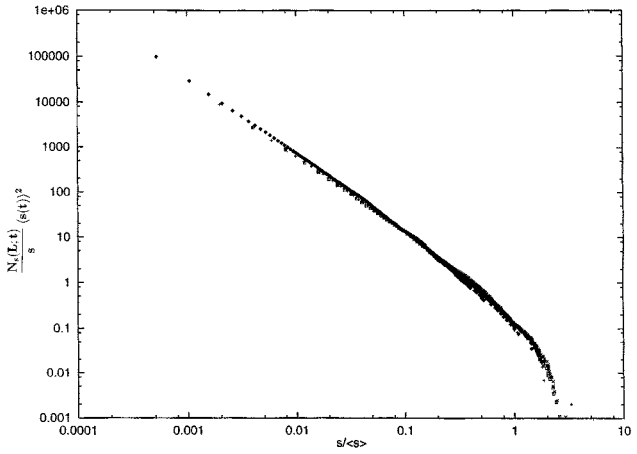


**Figure 22. Data collapse for the WF in an $L \times 2L$ square network at an intermediate time during FFD preceded by imbibition.**

The results are for $L = 100$ (diamonds), $L = 50$ (+), $L = 30$ (squares), $L = 20$ (×), $C = 10^{-5}$, and $f_w = 0.25$.

We also find that for a fixed $L$, and after some transient time, the data for various times can be collapsed onto a single curve according to

$$\frac{N_s(t;L)}{s} \sim \langle s\rangle^{-2} h[s(t)/\langle s(t)\rangle), \tag{14}$$

which is completely similar to Eq. 13, with $h(x)$ being another scaling function. For example, Figure 23 presents the results for the WF for $C = 10^{-5}$ in a $100 \times 200$ network during FFD preceded by imbibition and at several process times, indicating again very accurate data collapse. Equations 13 and 14 together indicate that $N_s(t, L)$ obeys a complete scaling law in both $t$ and $L$, which is an important characteristic of

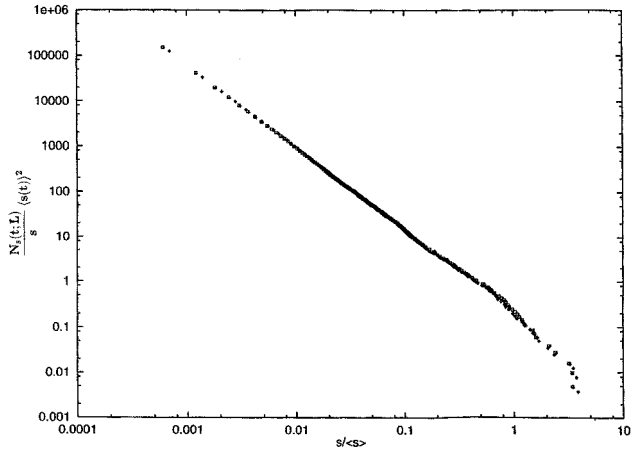


**Figure 23. Data collapse for the WF in a $100 \times 200$ square network during FFD preceded by imbibition.**

The results are at times $t = 8{,}000$ (diamonds), $t = 16{,}000$ (+), $t = 24{,}000$ (squares), $C = 10^{-5}$, and $f_w = 0.25$.

many dynamical processes (Family and Vicsek, 1991). This aspect of our model has been studied in detail elsewhere (Hashemi et al., 1999a).

## Summary and Conclusions

We have carried out an extensive study of a new model for two-phase flow and displacement in porous media in which the two fluids act both as the invading as well as the defending fluids. We find novel displacement patterns in which the cluster-size distribution of the two fluids, the mean cluster size, and the fluids' saturations all oscillate strongly with the process time. Such oscillations have been observed in experimental studies, but have mostly been attributed to the uncertainties in the experimental measurements. Our study, together with the work of Constantinides and Payatakes (1996), provides a physical explanation for such fluctuations and oscillations in terms of the dynamic breakup and recoalescence of the fluid clusters.

In this article we were concerned only with the dynamics of the displacement process and the shapes of the displacement patterns, but ignored the effect of the viscous forces, except those in the thin WF films. Elsewhere (Hashemi et al., 1999b) we calculate the pressure distributions in the two fluids during FFD, from which the relative permeabilities are calculated as functions of the capillary number, the ratio of the viscosities of the two fluids, and $f_w$, which is an important problem in the petroleum industry.

## Acknowledgments

This work was supported in part by the Petroleum Research Fund, administered by the American Chemical Society, and by the Ministry of Culture and Higher Education of Iran. We thank Dietrich Stauffer for many stimulating discussions and for his warm hospitality during the time that M. H. spent at Cologne University.

## Literature Cited

Avraam, D. G., G. B. Kolonis, T. C. Roumeliotis, G. N. Constantinides, and A. C. Payatakes, "Steady-State Two-Phase Flow through Planar and Non-Planar Model Porous Media," *Transp. Porous Media*, **16**, 75 (1994).

Avraam, D. G., and A. C. Payatakes, "Flow Regimes and Mechanisms of Steady-State Two-Phase Flow in Porous Media," *J. Fluid Mech.*, **293**, 207 (1995).

Birovljev, A., L. Furuberg, J. Feder, T. Jøssang, K. J. Måløy, and A. Aharony, "Gravity Invasion Percolation in Two-Dimensions: Experiment and Simulation," *Phys. Rev. Lett.*, **67**, 584 (1991).

Blunt, M. J., M. J. King, and H. Scher, "Simulation and Theory of Two-Phase Flow in Porous Media," *Phys. Rev. A*, **46**, 7680 (1992).

Blunt, M. J., and P. R. King, "Relative Permeabilities from Two- and Three-Dimensional Pore Scale Network Modelling," *Transp. Porous Media*, **6**, 407 (1991).

Blunt, M. J., and H. Scher, "Pore-Level Modeling of Wetting," *Phys. Rev. E*, **52**, 6387 (1995).

Bryant, S., and M. J. Blunt, "Prediction of Relative Permeability in Simple Porous Media," *Phys. Rev. A*, **46**, 2004 (1992).

Chandler, R., J. Koplik, K. Lerman, and J. F. Willemsen, "Capillary Displacement and Percolation in Porous Media," *J. Fluid Mech.*, **119**, 249 (1982).

Chatzis, I., and F. A. L. Dullien, "Modelling Pore Structure by 2-D and 3-D Networks with Applications to Sandstones," *J. Can. Pet. Technol.*, **16**, 97 (1977).

Chatzis, I., and F. A. L. Dullien, "The Modelling of Mercury Porosimetry and Relative Permeability of Mercury in Sandstones Using Percolation Theory," *Int. Chem. Eng.*, **25**, 47 (1985).

Cieplak, M., and M. O. Robbins, "Influence of Contact Angle on Quasistatic Fluid Invasion of Porous Media," *Phys. Rev. B*, **41**, 11508 (1990).

Constantinides, G. N., and A. C. Payatakes, "A Theoretical Model of Collision and Coalescence of Ganglia in Porous Media," *J. Colloid Interf. Sci.*, **141**, 486 (1991).

Constantinides, G. N., and A. C. Payatakes, "Network Simulation of Steady-State Two-Phase Flow in Consolidated Porous Media," *AIChE J.*, **42**, 369 (1996).

Craig, F. F., *The Reservoir Engineering Aspects of Waterflooding*, Society of Petroleum Engineers, Richardson, TX (1971).

Dias, M. M., and A. C. Payatakes, "Network Models for Two-Phase Flow in Porous Media: 1. Immiscible Microdisplacement of Non-Wetting Fluids," *J. Fluid Mech.*, **164**, 305 (1986a).

Dias, M. M., and A. C. Payatakes, "Network Models for Two-Phase Flow in Porous Media: 2. Motion of Oil Ganglia," *J. Fluid Mech.*, **164**, 337 (1986b).

Family, F., and T. Vicsek, *Dynamics of Fractal Surfaces*, World Scientific, Singapore (1991).

Furuberg, L., J. Feder, A. Aharony and T. Jøssang, "Dynamics of Invasion Percolation," *Phys. Rev. Lett.*, **61**, 2117 (1988).

Glass, R. J., and M. J. Nicholl, "Quantitative Visualization of Entrapped Phase Dissolution Within a Horizontal Flowing Fracture," *Geophys. Res. Lett.*, **22**, 1413 (1995).

Glass, R. J., M. J. Nicholl, and V.C. Tidwell, "Challenging Models for Flow in Unsaturated, Fractured Rock Through Exploration of Small Scale Processes," *Geophys. Res. Lett.*, **22**, 1457 (1995).

Glass, R. J., and D. L. Norton, in, *Proc. 3rd Ann. Int. Conf. on High Level Radioactive Waste Management*, American Nuclear Society, Las Vegas, p. 717 (1992).

Goode, P. A., and T. S. Ramakrishnan, "Momentum Transfer Across Fluid-Fluid Interfaces in Porous Media: A Network Model," *AIChE J.*, **39**, 1124 (1993).

Hashemi, M., M. Sahimi, and B. Dabir, "Percolation with Two-Invaders and Two-Defenders: Volatile Clusters, Oscillations, and Scaling," *Phys. Rev. Lett.*, **80**, 3248 (1998).

Hashemi, M., M. Sahimi, and B. Dabir, "Monte Carlo Simulation of Two-Phase Flow in Porous Media: Invasion with Two Invaders and Two Defenders," *Physica A*, **267**, 1 (1999a).

Hashemi, M., B. Dabir, and M. Sahimi, "Network Simulation of Relative Permeabilities and Fractional Flows," *Transp. Porous Media* (1999b).

Heiba, A. A., H. T. Davis, and L. E. Scriven, "Effect of Wettability on Relative Permeabilities and Capillary Pressures," Society of Petroleum Engineers Paper 12172 (1983).

Heiba, A. A., H. T. Davis, and L. E. Scriven, "Statistical Network Theory of Three-Phase Relative Permeabilities," Society of Petroleum Engineers Paper 12690 (1984).

Heiba, A. A., M. Sahimi, L. E. Scriven, and H. T. Davis, "Percolation Theory of Two-Phase Relative Permeability and Capillary Pressure," Society of Petroleum Engineers Paper 11015 (1982).

Heiba, A. A., M. Sahimi, L.E. Scriven, and H.T. Davis, "Percolation Theory of Two-Phase Relative Permeabilities," *SPE Reservoir Eng.*, **7**, 123 (1992).

Kantzas, A., and I. Chatzis, "Network Simulation of Relative Permeability Curves Using a Bond Correlated-Site Percolation Model of Pore Structure," *Chem. Eng. Commun.*, **69**, 191 (1988).

Koplik, J., and T. J. Lasseter, "Two-Phase Flow in Random Network Models of Porous Media," *Soc. Pet. Eng. J.*, **25**, 89 (1985).

Larson, R. G., L. E. Scriven, and H. T. Davis, "Percolation Theory of Residual Phases in Porous Media," *Nature*, **268**, 409 (1977).

Larson, R. G., H. T. Davis, and L. E. Scriven, "Percolation Theory of Two-Phase Flow in Porous Media," *Chem. Eng. Sci.*, **36**, 57 (1981).

Lenormand, R., and S. Bories, "Description d'un Mécanisme de Connexion de Liaisons Destiné a L'étude du Drainage avec Pigéage en Milieu Poreux," *C. R. Acad. Sci. Paris*, **B291**, 279 (1980).

Lenormand, R., E. Toubol, and C. Zarcone, "Numerical Models and Experiments on Immiscible Displacements in Porous Media," *J. Fluid Mech.*, **189**, 165 (1988).

Lenormand, R., C. Zarcone, and A. Sarr, "Mechanisms of Displacement of One Fluid by Another in a Network of Capillary Ducts," *J. Fluid Mech.*, **135**, 637 (1983).

Martys, N., M. Cieplak, and M. O. Robbins, "Critical Phenomena in Fluid Invasion of Porous Media," *Phys. Rev. Lett.*, **66**, 1058 (1991).

Mohanty, K. K., H. T. Davis, and L. E. Scriven, ''Physics of Oil Entrapment in Water-Wet Rock,'' *SPE Reservoir Eng.*, **2**, 113 (1987).
Moreno, L., Y. W. Tsang, C. F. Tsang, F. V. Hale, and I. Neretnieks, ''Flow and Tracer Transport in a Single Fracture: A Stochastic Model and Its Relation to some Field Observations,'' *Water Resour. Res.*, **24**, 2033 (1988).
Ransohoff, T. C., and C. J. Radke, ''Laminar Flow of a Wetting Liquid along the Corners of a Predominantly Gas-Occupied Noncircular Pore,'' *J. Colloid Interf. Sci.*, **121**, 392 (1988).
Sahimi, M., ''On the Determination of Transport Properties of Disordered Systems,'' *Chem. Eng. Commun.*, **64**, 179 (1988).
Sahimi, M., ''Flow Phenomena in Rocks: From Continuum Models to Fractals, Percolation, Cellular Automata and Simulated Annealing,'' *Rev. Mod. Phys.*, **65**, 1393 (1993).
Sahimi, M., *Applications of Percolation Theory*, Taylor & Francis, London (1994).
Sahimi, M., *Flow and Transport in Porous Media and Fractured Rock*, VCH, Weinheim, Germany, 1995).
Stauffer, D., and A. Aharony, *Introduction to Percolation Theory*, 2nd ed., Taylor & Francis, London (1992).
Wilkinson, D., and J. F. Willemsen, ''Invasion Percolation: A New Form of Percolation Theory,'' *J. Phys. A*, **16**, 3365 (1983).

*Manuscript received Jun. 26, 1998, and revision received Apr. 9, 1999.*